

point of view of the electrons and their interactions, and completely disregards their wave aspect. The agreement between theory and experiment may justify this in the case of helium. We have plenty of evidence, however, from electron diffraction effects that the elastic electron scattering does require us to use the wave aspect for a complete description of what happens. This raises the question as to whether or not it is necessary to modify the method of using the experimental data described in the earlier paper so as, in some way, to take account

of the wave nature of the electrons in the inelastic electron scattering. We are inclined to think, however, that the simple particle view can be retained in the interpretation of this kind of experiment, and that the discrepancy will be removed by a more accurate method of handling the wave mechanical description of the hydrogen molecule.

We wish to thank Professor Kirkpatrick and Dr. Hicks for letting us have the numerical values from which their published curves were drawn.

AUGUST 1, 1938

PHYSICAL REVIEW

VOLUME 54

A New Precision Method for the Determination of e/m for Electrons

A. E. SHAW

Ryerson Physical Laboratory, University of Chicago, Chicago, Illinois

(Received June 10, 1938)

The excellent focusing properties of crossed electric and magnetic fields have been utilized in the development of a new, precision method for the determination of e/m for electrons. This method differs from previous methods in that the final equation for e/m does not involve the velocity explicitly. Moreover, focusing criteria have been worked out which effectively eliminate any possible influence of electron energy upon the value of e/m . That this is a great source of error and uncertainty in other methods is shown by the great difference between the energy of the electrons before and after emergence from a slit. This effect is too great to arise from a contact potential difference but it can be attributed to direct electron bombardment of the slit and the subsequent formation of a surface charge on it. The magnitude of this charge is not constant but varies between 9 volts and 24 volts, depending upon the applied accelerating potential. The value of e/m obtained with the

present apparatus is, $e/m_0 = (1.7571 \pm 0.0013) \times 10^7$ e.m.u., where 0.0013 is the probable error derived from a least squares solution of a set of observations for various electric and magnetic field intensities. Other sets differed from this by less than 1 : 5000. The mechanical accuracy of the present cylindrical condenser sets the limit on the precision attainable with the present apparatus. However, the error due to this cause is less than the probable error stated above. The limitations of the present condenser can be reduced considerably through the use of a new condenser designed in accordance with kinematic principles. The method presented here for the production of magnetic fields of great uniformity and a new, precise cylindrical condenser would permit a determination of e/m to be made with the method of crossed fields to within an accuracy of 1 : 3000.

I. INTRODUCTION

THE focusing properties of crossed electric and magnetic fields for electrons, in the case of circular orbits, were discussed in a recent¹ paper in this journal. It was found that this combination of fields is capable of extremely sharp focusing of electron beams that vary both in direction and in velocity.

This same field combination was investigated experimentally to determine its suitability for

the accurate measurement of the specific charge of electrons. In practically all deflection measurements of e/m , the precision is limited by uncertainties in the velocity of the electrons. In the method of crossed fields, the final equation does not contain the velocity explicitly, hence uncertainties in the accelerating potential do not enter. Although the accelerating potential does not appear explicitly in the equation for e/m , provision must be made by focusing to adjust the velocity for any given ratio of intensities of the electric and magnetic fields.

¹ A. E. Shaw, Phys. Rev. **44**, 1006 (1933).

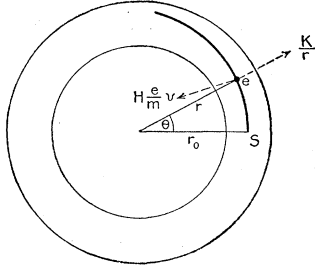


FIG. 1. Section through cylindrical condenser showing the accelerations of an electron in crossed electric and magnetic fields.

The aim of the present paper is: (1) to describe experimental focusing criteria which eliminate the velocity uncertainty from the method of crossed fields, and: (2) to present the details of the measurement of e/m by this new method.

II. THEORY OF METHOD

In Fig. 1 is shown a schematic representation of a cylindrical condenser in which a beam of charged particles is free to move under the action of a radial electric field and a magnetic field which is normal to the plane of the orbit.

A charged particle entering the field at S describes an orbit under the influence of a radial acceleration K/r due to the electric field, and of an acceleration $(He/m)v$, due to the magnetic field which acts at right angles to its direction of motion at every point of the orbit. If the direction of the two forces are as shown, the equations of motion in polar coordinates are,²

$$r'' - r(\theta')^2 = K/r - (He/m)r\theta', \quad (1)$$

$$(r^2\theta')'/r = (He/m)r', \quad (2)$$

where the primes indicate time derivatives. Eq. (2) can be written $(r^2\theta')' = \frac{1}{2}(He/m) \cdot (r^2)'$, which, integrated subject to the initial conditions that at $t=0$; $r=r_0$, $r'=r_0'$, $\theta=0$ and $\theta'=\theta_0'$ gives $\theta' = \frac{1}{2}(He/m) + A/r^2$, where $A = r_0^2[\theta_0' - \frac{1}{2}(He/m)]$. Substituting this value of θ' into Eq. (1), there results,

$$r'' = A^2/r^3 + K/r - r(\frac{1}{2}He/m)^2. \quad (3)$$

We are interested only in those orbits which are nearly circular, since only these may be

² W. Bartky and A. J. Dempster, Phys. Rev. **33**, 1019 (1929). Cf. also J. Mattauich and R. Herzog, Zeits. f. Physik **89**, 786 (1934).

described in the condenser under consideration. For the circular orbit $r=\rho$, a constant, the magnetic force is always directed along the radius vector, hence Eq. (3) becomes,

$$A^2/\rho^4 = (\frac{1}{2}He/m)^2 - K/\rho^2. \quad (4)$$

For orbits which differ by an amount x from a circle, $r=\rho$, let $r=\rho+x$, then Eq. (3) can be written,

$$x'' = -x[(He/m)^2 - 2K/\rho^2]. \quad (5)$$

If the electric and magnetic fields and the initial angular velocity θ_0' are adjusted so that $A=0$, then from Eq. (4), $(He/m)^2 = 4K/\rho^2$ and Eq. (5) becomes,

$$x'' = -\frac{1}{2}(He/m)^2x \quad (6)$$

and

$$\theta' = \frac{1}{2}(He/m). \quad (7)$$

The solution of Eq. (6) is

$$x = P \sin (He/m)t/\sqrt{2}. \quad (8)$$

The beam is focused when $x=0$; thus it is evident from Eq. (8) that a divergent bundle of rays is reunited after a time $t = \pi\sqrt{2}/(He/m)$. The angular distance traversed by the beam in this time t is obtained from the solution of Eq. (7). It is $\pi/\sqrt{2}$ radians, or $127^\circ 17'$.

If r be substituted for ρ in Eq. (1) and ρ be considered a function of θ' , we find that ρ passes through a minimum for $\theta' = \frac{1}{2}He/m$. Therefore, when the adjustment of the electric and magnetic fields is such as to make $A=0$ and $(He/m)^2 = 4K/\rho^2$, we have particles with slightly different velocities describing approximately the same circular orbit.

To find the sharpness of focus, the orbits described by the particles having different directions and different velocities can be computed to a further approximation,² which gives a general equation for the radius vector of the path at the point of focus; viz., $\theta = 127^\circ 17'$ as follows:

$$r = \rho(1 - c_0 + c_0^2/3 + c_1^2/3 + \delta^2 + \pi c_1 \delta/\sqrt{2}). \quad (9)$$

This equation contains the initial conditions associated with the entering slit, that is where $\theta=0$, we have for the point of entry, $r_0 = \rho(1 + c_0)$, and for the angle of entry, $(dr/pd\theta)_{\theta=0} = c_1$, and for the angular velocity at entry, $(d\theta/dt)_{\theta=0} = \frac{1}{2}H(1 + \delta)e/m$.

Since Eq. (9) is quadratic in δ it shows that there are in general two values of the velocity to give any r . For a beam of small angular divergence $c_1=0$ and these two values coincide at a minimum value for $\delta=0$. Thus at $\theta=\pi/\sqrt{2}$, $r=\rho(1-c_0+c_0^2/3)$, where ρ is expressed by the relation,

$$\rho^2 = 4K/(He/m)^2. \quad (10)$$

In the apparatus, c_0 was of the order of 0.00026, so that $\rho = \frac{1}{2}(r_0+r)$ to better than 1 : 10⁶.

In the event that c_1 , the angle of entry at $\theta=0$, is not zero, the minimum value of the radius at $\theta=\pi/\sqrt{2}$, as δ is varied, is found from Eq. (9) to be $r = \rho(1 - c_0 + c_0^2/3 - 0.9c_1^2)$, so that $\frac{1}{2}(r_0+r) = \rho(1 + c_0^2/6 - 0.45c_1^2)$ is the equation that connects ρ with the observed values of r_0 and r . The term $c_0^2/6$ is less than 1 : 10⁶ hence it can be neglected. In several preliminary tests sufficient gas was admitted to make the electron beam visible. It was then seen to be a sharp bundle down the center of the condenser with a maximum divergence of less than 1 : 50. Thus the term $0.45c_1^2$ is less than 1 : 6000 for the rays of maximum divergence and the change in ρ is less than 1 : 6000.

In the experimental realization of these condi-

tions, either the electric field or the magnetic field is adjusted so that the beam is focused onto the collector at r , as a minimum value for variations of the velocity. Then from the value of ρ , e/m can be computed from $(e/m)^2 = 4K/H^2\rho^2$. The value of K may be deduced from the equation,

$$m \int_{r=r_1}^{r_2} \frac{K}{r} dr = eV, \quad (11)$$

where r_1 and r_2 represent respectively the radii of curvature of the inner and outer plates of the condenser and V is the potential difference across the condenser. The value of K from Eq. (11), when combined with Eq. (10) gives,

$$e/m = \frac{4V}{H^2\rho^2 \log_e (r_2/r_1)}. \quad (12)$$

Thus we have an expression for e/m in terms of the electrostatic field intensity, the magnetic field intensity and the radius of curvature of the electron beam.

III. GENERAL EXPERIMENTAL ARRANGEMENT

The schematic diagram of the entire apparatus is shown in Fig. 2, where the cylindrical con-

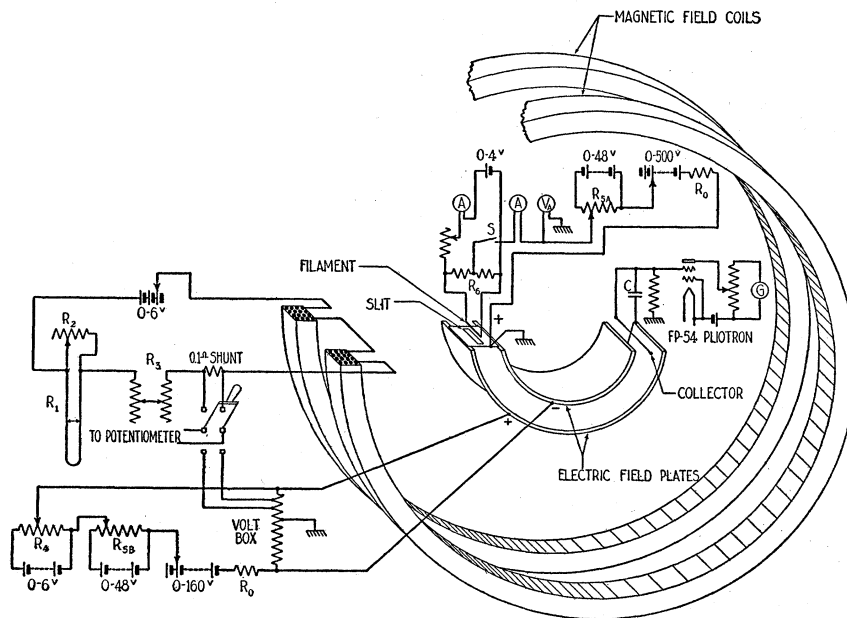


FIG. 2. Schematic diagram of the control circuits for the electric field, the magnetic field, the accelerating field and the electron collector.

denser and the magnetic field coils are represented in oblique projection.

(A) Source of electrons

The source of electrons was a coated cylindrical filament, 0.025 mm in diameter. The filament was mounted like a monochord string under the slight tension of a tungsten-molybdenum spring (T in Fig. 3) in order that its expansion when heated would not throw it out of the line of the slit. The tungsten-molybdenum spring was shunted by a flexible strip of pure silver which carried most of the heating current. The filament gave adequate emission when heated by currents of approximately 0.050 ampere. Although the filament support and its circuit were almost non-inductive, the small heating currents served to minimize its magnetic field.

The activation of the filament required a heating current of 0.1 ampere and an accelerating potential of 350 volts. This process was carried out in a separate evacuated chamber outside of the main apparatus. When the filament was properly activated, it was mounted in its support and installed in the apparatus. In this way it was possible to retard the formation of partially insulating layers on the surface of the slit (S in Fig. 3) adjacent to the filament. It was found necessary to shield the filament on all sides in order to restrict the electrons to the slit.

(B) Slit

The photograph in Fig. 3 shows the slit, the collector and the inner plate of the cylindrical condenser. The slit S which collimated the electron beam, was 0.03 mm wide and 2.0 mm long. The plate in which the slit was formed was made of gold to avoid surface oxidation under electron bombardment. The slit was located symmetrically with respect to the two plates of the cylindrical condenser and its plane was radial. The radial position of the slit was set by means of a mechanical fixture which fitted over the inner plate of the cylindrical condenser. There was no electrostatic deflecting field in the region between the filament and the slit (see Figs. 2 and 4). It was necessary, therefore, to place the filament in such a position that the electrons, under the influence of the accelerating field and the magnetic field, entered the slit normally.

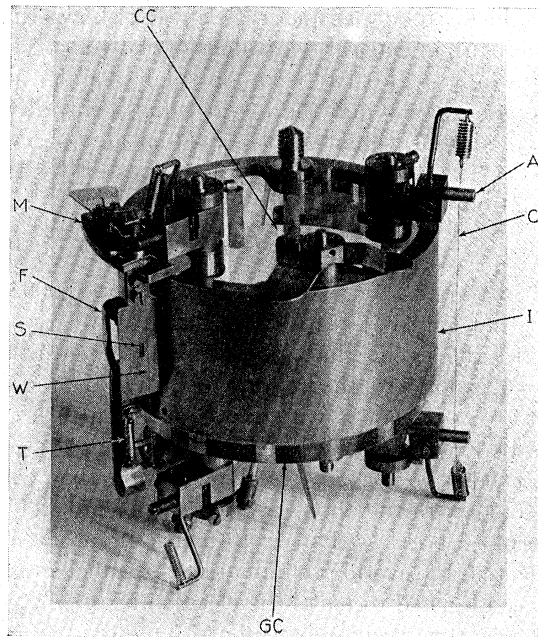


FIG. 3. Inner plate of cylindrical condenser, showing collector and slit system. C , gold wire collector, 0.045 mm diameter; A , 0.1 mm pitch adjusting screw; I , inner plate of cylindrical condenser; GC , accurate glass cylinder; CC , center of curvature of plates engraved on front face of GC ; S , slit for beam, 0.03×2.0 mm; M , mechanism for adjusting slit; W , old wire slit, no longer used; F , filament support. Filament is directly in back of S ; T , spring to compensate for expansion of filament.

The wire slit (W in Fig. 3), mentioned in an earlier paper,¹ served originally as the initial slit, the image of which was focused onto the collector. This wire slit has been abandoned because of difficulty with surface charges forming on it. The final readings presented in this paper were taken with the wire slit removed. The angle of refocus, namely $127^\circ 17'$, was measured between slit S and the collector, since the distortion of the radial field in the vicinity of the slit has a negligible effect on the position of focus.

(C) Accelerating field

The control circuit for the accelerating field is shown in Fig. 2. The accelerating potential was applied between the grounded slit and the midpoint of two 150,000 ohm resistances, R_6 . The accelerating potential was read³ on voltmeter V_A ,

³ The small drop due to the emission current was approximately 0.03 volt.

which was a precision instrument of one megohm. Resistance R_{5A} was a 2500 ohm slide-wire and R_0 was a 5000 ohm protective resistance. All potentials were supplied by storage cells to insure constancy.

Switch S provided an important control for the accelerating field. It was open while the electric and magnetic field circuits were being adjusted. Thus, in addition to minimizing the bombardment of the slit, the electrons from the filament were kept out of the cylindrical condenser until the electrostatic and the magnetic forces were adjusted approximately to bend them into a circular orbit. This same procedure was followed for each new set of values of the electric and magnetic fields.

(D) Collector

The electron beam was picked up by a cylindrical gold wire, 0.045 mm diameter (C in Fig. 3) which was connected to an FP 54 Pliotron,⁴ as shown in Fig. 2. The current sensitivity of this circuit was of the order of 10^{-14} ampere and electron currents to the collector were of the order of 2×10^{-11} ampere.

The wire type of collector was chosen in order to avoid distortion of the radial electric field. One interesting feature of the use of a wire collector was the fact that the ratio of secondary electrons to primary electrons was greater than unity, thus giving the wire a net positive charge. This was verified by the use of a small Faraday chamber consisting of two coaxial tubes, the inner of which was joined to the Pliotron. With this arrangement, the secondary electrons were not able to escape and the collecting circuit showed a net negative charge. There appears to be no effective way of eliminating secondary emission under these circumstances, hence focusing was carried out in terms of a positive deflection. When operating at pressures of the order of 10^{-7} mm Hg, and small beam intensities, the deflections were very constant. It is also important to note that with the beam intensities used, no appreciable change, due to electron bombardment, took place on the surface of the collector, for long periods of time.

Although the collector was located symmetrically with respect to the two plates of the cylindrical condenser, it was not electrostatically symmetrical because of its two supports. Thus when the potential across the electric field plates was varied, a charge was induced in the Pliotron circuit. Condenser C (Fig. 2) of air dielectric and capacity $2.48 \mu\mu\text{f}$, established the electrostatic symmetry of the collector and eliminated the induced charge.

The adjustment of the collector with respect to angle and radius was carried out by means of the mechanism shown in Fig. 3. A was a 0.1 mm pitch screw of which there were two. These screws possessed one degree of freedom in rotation and their supports one degree of freedom in angle. This allowed the collector to be located at the proper angular distance from the slit and at the appropriate radius of curvature. The accuracy with which this angle may be set does not influence appreciably the ultimate precision of the determination. The method employed in the final measurement of the radius of curvature will be described in the section on the electric field.

(E) Electric field

(a) *Mechanical structure and physical measurement.*—The electric field was formed between two concentric cylindrical surfaces which were held concentric by means of an accurately turned glass cylinder (GC in Fig. 3). Upon the front face of this cylinder was engraved the center of curvature (CC in Fig. 3). The effective axial length of the electric field was about 3.0 cm whereas the axial width of the electron beam was only 0.2 cm.

The field plates were cast from a bronze whose magnetic susceptibility was checked by a sensitive method⁵ and found to be negligibly small. After careful machining, each plate was coated electrolytically with a layer of 24-carat gold, in order to minimize the polarization described later.

The radii of curvature of the two cylindrical condenser plates were 3.4071 cm and 2.7901 cm. These dimensions were determined in the follow-

⁴ L. A. DuBridge, Phys. Rev. **37**, 392 (1931).

⁵ E. B. Rosa, *et al.*, Bull. Nat. Bur. Stand. **8**, 285 (1912). Cf. also Jackson, Proc. Roy. Soc. A104, 672 (1923) for absolute method of calibration.

ing manner. First the diameter of the inner plate was measured in various azimuths by means of a Swedish Gage Company micrometer caliper. This micrometer, of grade *A*, was checked against its standard block at frequent intervals. The two cylindrical plates were assembled in their final position with respect to the glass cylinder and bolted together securely. This unit was then placed on the bed of a Geneva comparator in a fixture that permitted one degree of rotation about the axis of the glass cylinder which was perpendicular to the bed. An accurate steel sphere, coated with a thin layer of 24-carat gold, was attached to the end of a tool steel rod of diameter smaller than the sphere. The steel rod was arranged vertically so that the sphere, which was fastened to the lower end of the rod, lay between the two condenser plates. The support holding the sphere was independent of the bed of the comparator, and thus a translation of the bed of the comparator moved the condenser plates with respect to the sphere.⁶ The sphere and the two plates were joined together in a simple electrical circuit in such a way that contact between the sphere and either of the plates

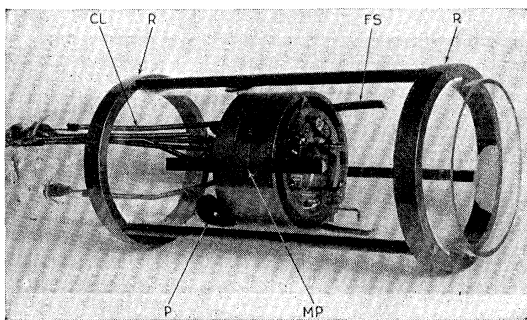


FIG. 4. Cylindrical condenser in glass tube. End plate removed. *CL*, spring connecting leads; *R*, ring supports; *MP*, median plane of electron beam; *P*, round glass pins that hold condenser in median plane under force of spring leads; *FS*, flat spring, of which there are six, to support condenser in glass tube.

⁶ It is assumed that the relative motion of the cylindrical plates and the sphere is along a diametral line. However, it can be shown that, even if the line of motion were not coincident with a diametral line by as much as 0.5 mm, the corresponding error in the measurement of the separation would not exceed 1 : 8000. This can be inferred from the equation,

$$Y = (r_2 - r_1) \left[1 + \frac{1}{2} \left(\frac{X^2}{r_1 r_2} \right) + \dots \right],$$

where Y is the separation of the two cylindrical surfaces of radii r_1 and r_2 , measured along a line parallel to a diametral line but removed from it by a perpendicular distance X .

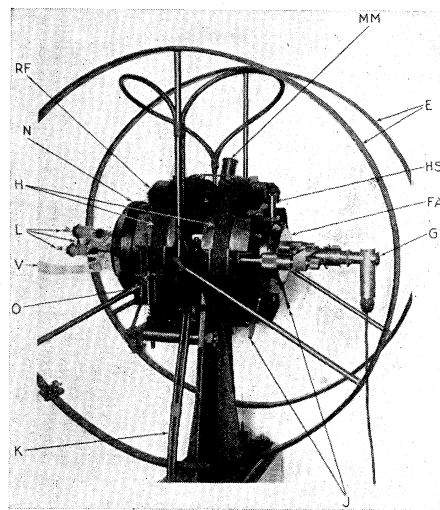


FIG. 5. Complete assembly of the entire apparatus with measuring microscopes in place. *FA*, glass tube containing cylindrical condenser; *E*, coils for investigating influence of earth's field; *GE*, combination Gauss eyepiece and telescope for locating cylindrical condenser; *J*, thumb screws to adjust position of cylindrical condenser—there are two in front and two in rear; *HS*, spring plunger which maintains glass tube (*FA*) in contact with thumb screws (*J*); *N*, nut to translate glass tube (*FA*) along axis of magnetic field; *MM*, median plane microscope to judge coincidence of median planes; *H*, magnetic field coils; *K*, noninductive connections to magnetic field coils; *RF* heat radiating fins; *L*, external leads for connections to cylindrical condenser, filament, etc.; *V*, vacuum pump connection; *O*, magnetometer mounted externally to indicate presence of stray fields.

was indicated on a galvanometer. In this manner, careful measurements were made of the radial separation of the condenser plates in the median plane of the electron beam in four different azimuths between the slit and the collector wire. This method of measuring the actual separation between two cylindrical surfaces is capable of precision and reproducibility.

In measuring the width of a slot by the motion of a sphere, no lost motion due to backlash in gears is permissible. This was avoided in the Geneva comparator through the use of an Ames dial gauge which was attached to the end of the comparator in contact with the bed. Thus the screw of the comparator served merely to translate the plates whose separation was desired. By choosing a measuring sphere of proper diameter, the displacement of the dial gauge was limited, thereby minimizing the slight periodic error due to the eccentricity of the pinion in the gauge. Finally, the dial gauge was calibrated against our

decimeter standard No. 56 which had recently⁷ been checked by the National Bureau of Standards. The gold plated sphere was measured in a number of azimuths by means of an accurate micrometer caliper.

The precise location of the collector wire was determined by a slight modification of the foregoing method. The wire was connected electrically to the inner plate and thence through the galvanometer circuit to a gold plated sphere as before. In this way the wire was located with respect to the inner plate. However, one very important precaution is to be observed, that is, the wire must always contact the sphere at the end of that diameter of the sphere which lies along the line of the displacement. If the sphere were out of line on either side, the actual displacement would be greater, hence by rotating the condenser plates with respect to the sphere through a very small angle about their vertical axis, a minimum displacement of the sphere between the inner plate and the collector wire can be found. A number of such readings were taken first at a point below the median plane of the electron beam and then at a corresponding point above the median plane. This enabled the wire to be located parallel to an element of the inner cylindrical surface in the proper radial position.

The complete cylindrical condenser with filament, slit and collector installed and measured was mounted inside a glass tube, as shown in Fig. 4. This glass tube fits inside the magnetic field coils as indicated in Fig. 5. The two rings R (Fig. 4) were supported in the magnetic field coils on six points, four of which were rigid (J in Fig. 5) and two of which were flexible (HS in Fig. 5). The front flexible support, which consisted of a bronze helical spring was coupled to the ring R through a ball and socket, thus applying two degrees of constraint in translation. This method of mounting the glass tube inside the field coils provides three degrees of freedom in angle and one degree in translation. In addition, the nut N (Fig. 5) gives one degree in translation. This combined motion enabled the cylindrical condenser to be located symmetrically inside the magnetic field.

⁷L. V. Judson and B. L. Page, Nat. Bur. Stand. J. Research **13**, 757 (1934).

The actual location of the cylindrical condenser was accomplished by the use of a combination Gauss eyepiece and telescope (GE Fig. 5). The Gauss eyepiece was used to establish the plane of the trajectory normal to the magnetic field. After this, the telescopic objective was attached and the center of curvature of the cylindrical plates was located on the axis of the magnetic field. The reference plane for these adjustments was the polished front face of the glass cylinder (GC in Fig. 3). The microscope, MM in Fig. 5 was used to judge the coincidence of the median plane of the electron beam with the common median plane of the two magnetic field coils.

(b) *Electrical control circuits.*—The electric circuit which controls the electrostatic deflecting field is shown in Fig. 2. Rheostat R_1 consisted of a single layer of resistance wire wound in a helical groove on the surface of a cylinder. The cylinder was capable of rotation and a moving contact slid over every portion of the helical winding when the cylinder was turned about its axis. This provided a continuously variable potential for the fine adjustment of the electric field. The coarse adjustment was made by means of the slide wire R_{5B} and the switch attached to the 0–160 volt storage battery. The volt box⁸ shown was used to measure the potentials applied to the electric field.

The slit and the wire collector were located practically midway between the two plates of the cylindrical condenser. In some of the preliminary experiments, the zero equipotential surface, containing the slit and the collector was also located midway by making $V_1 \neq V_2$. If we let r_1 and r_2 be respectively the radii of the inner and the outer plates of the cylindrical condenser, then ;

$$eV_1 = m \int_{r=r_1}^{r_1 + \frac{1}{2}(r_2 - r_1)} \frac{K}{r} dr$$

$$\text{and } eV_2 = m \int_{r_1 + \frac{1}{2}(r_2 - r_1)}^{r_2} \frac{K}{r} dr.$$

Experimentally, no observable difference was

⁸This was a Leeds and Northrup volt box that had been checked at the National Bureau of Standards and more recently had been rechecked along with the 0.1 ohm standard in the Standards Laboratory of the Commonwealth Edison Company, Chicago, through the courtesy of Mr. Stevens and Mr. Dondanville.

found between the adjustment for focus when these values of V were used and the adjustment when V_1 was made equal to V_2 . The ground on the voltbox in Fig. 2 was the connection that established the zero surface.

(F) Magnetic field

(a) *Mechanical structure and electrical circuits.*—The magnetic field which was used to deflect the electron beam was produced by the two coils shown at H in Fig. 5. The coils were rectangular in cross section and each was composed of 119 turns of No. 12 Cotenamyl wire, thoroughly shellacked. Each coil was wound on a bronze frame which slid without shake over an accurately turned cylinder of bronze. The coil frames were attached to the cylinder by three point screw supports in such a manner that the separation and the parallelism of the two coils could be adjusted with considerable accuracy. The coils were so arranged on their cylindrical support that when their individual median planes were parallel to each other, the magnetic axis of one coil was coincident with the magnetic axis of the other.

The determination of the constant of the magnetic field coils was made by means of the two standard coils shown in the schematic diagram of Fig. 6. Standard coil No. 1 consisted of two single layer coils of seven turns each of No. 12 enameled copper wire. The wire was wound in an 80° helical groove of pitch slightly greater than the diameter of the wire. These two coils were wound on the central portion of the cylinder, at the ends of which were located the two magnetic field coils. Standard coil No. 1 and the magnetic field coils were coaxial about axis A . For simplicity in representation, several turns have been omitted from the drawing of coil No. 1 in Fig. 6. The two coils of standard No. 1 were connected in series aiding and the two magnetic field coils were also series aiding.

The field of standard No. 1 was arranged to oppose the field of the magnetic field coils. The glass assembly shown in Fig. 4 was removed and a small oil-damped magnetometer, whose motion was magnified optically, was placed at a point which lay on the trajectory. This indicated when the two fields were equal. Equality was always judged for current reversals through both sets of

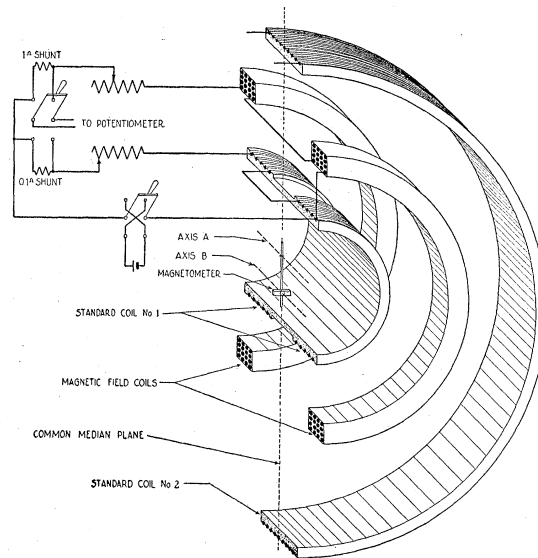


FIG. 6. Schematic diagram in section of the arrangement used for standardizing the magnetic field coils. The common median plane is parallel to plane of diagram.

coils, thus correcting for magnetic asymmetry, in the neighborhood of the coils. This null arrangement provided a simple, yet precise method for the determination of the constant of the magnetic field coils at the trajectory in terms of a standard coil. Since the plane of the trajectory was parallel to the plane of the magnetic meridian of the earth's field, as determined within the laboratory, it was unnecessary to compensate for the earth's field. From the spot finally formed on the collector after long bombardment, it may be concluded that the electrons were practically completely confined to the plane at right angles to the axis. Hence, with no component of motion normal to the plane of the orbit, the earth's field had no influence and spiralling was negligible.

The mathematical computation of the constant of standard No. 1 for points on the trajectory involved an infinite series. Although this series is rapidly convergent, it was nevertheless desirable to secure an additional experimental check of standard No. 1. This was accomplished by means of standard No. 2, also shown in Fig. 6. This standard, which could be attached to the assembly shown in Fig. 5, consisted of a single layer of 24 turns of No. 20 enameled copper wire. For simplicity, only a few turns are shown in the drawing. The wire was wound in an 80° helical

groove of pitch slightly greater than the diameter of the wire. The cylinder upon which this coil was wound was located so that the magnetic axis of the coil was coincident with axis B , which lay in the trajectory. That is to say, the radial distance between axes A and B was practically equal to the radius of the trajectory. Standard No. 2 could be utilized to compensate either standard No. 1, or the magnetic field coils. The procedure was identical in either case, and the magnetometer was used as before to indicate when the fields were equal.

The leads from the various coils were brought out in the plane which was normal to the common median plane (Fig. 6) in order to avoid the magnetic contributions of these short leads. The connecting wires to the control circuit were non-inductive. In order further to eliminate stray fields, any material which affected the magnetometer was removed from the vicinity of the apparatus. It was found that anything which was too far off to disturb the magnetometer had no observable effect on the electron beam. The slight stray fields due to the slide wires in the accelerating field and in the electric field circuits were eliminated by allowing currents to flow to them through noninductive leads from the battery. The slide wires were then moved about until the magnetometer showed no deflection, even for current reversals. The slide wires were then fastened permanently in their respective positions. This procedure was followed in locating all of the control apparatus. After all the apparatus had been placed and the fields measured, the magnetometer was mounted permanently in position O shown in Fig. 5. Even though this was removed from the region of the trajectory, it was found that stray fields incapable of affecting the magnetometer in this position had no effect on the electron beam.

The control circuit for the magnetic field coils is shown in Fig. 2. Rheostat R_3 was for the coarse adjustment whereas R_1 shunted by R_2 provided the fine adjustment, which was used in the actual focusing of the electrons. Rheostats R_1 and R_3 were practically noninductive. R_1 consisted of a narrow loop of manganin wire shunted by a slider of the same material. This provided a continuously variable adjustment. R_3 consisted of two ribbon wound coils adjacent to each other

with a common slider. The smallness of the current through R_2 and its remoteness from the main field made it unnecessary that it be noninductive.

The current for the magnetic field coils was supplied by large capacity lead storage cells and the absolute magnitude⁸ of the current was read on the same potentiometer that was used to measure the potential of the electric field.

(b) *Evaluation of intensity constants for standard coils.*—Many coils have been devised for the production of homogeneous magnetic fields. These range all the way from various combinations of conical and cylindrical solenoids to finite groups of windings, of which the Helmholtz arrangement is perhaps the best known. The Helmholtz combination produces a field of uniform intensity in the neighborhood of the magnetic axis and in the common median plane. The author has found it possible to produce a field of uniform intensity in the median plane but at any desired point off the axis by reducing the usual separation implied by the Helmholtz arrangement.

The x component of the magnetic field intensity in oersteds of a single circular turn of wire carrying current i (e.m.u.) is given by⁹

$$H_x = \frac{2\pi ia^2}{r^3} \left\{ 1 + \frac{3y^2}{2^2 r^4} (a^2 - 4x^2) + \frac{45y^4}{2^2 4^2 r^8} (a^4 - 12a^2 x^2 + 8x^4) + \frac{45y^6}{2^2 4^2 6^2 r^{12}} (35a^6 - 840a^4 x^2 + 1680a^2 x^4 - 448x^6) + \frac{15y^8}{2^2 4^2 6^2 8^2 r^{16}} (6615a^8 - 264,600a^6 x^2 + 1,058,400a^4 x^4 - 84,672a^2 x^6 + 120,960x^8) + \dots \right\}. \quad (13)$$

Here x and y represent the coordinates of the point at which H_x is expressed, with the origin of

⁹ A. Gray, *Absolute Measurements in Electricity and Magnetism*, second edition (1921), p. 212. The fifth term was derived by the author because of the insufficiently rapid convergence of the first four terms.

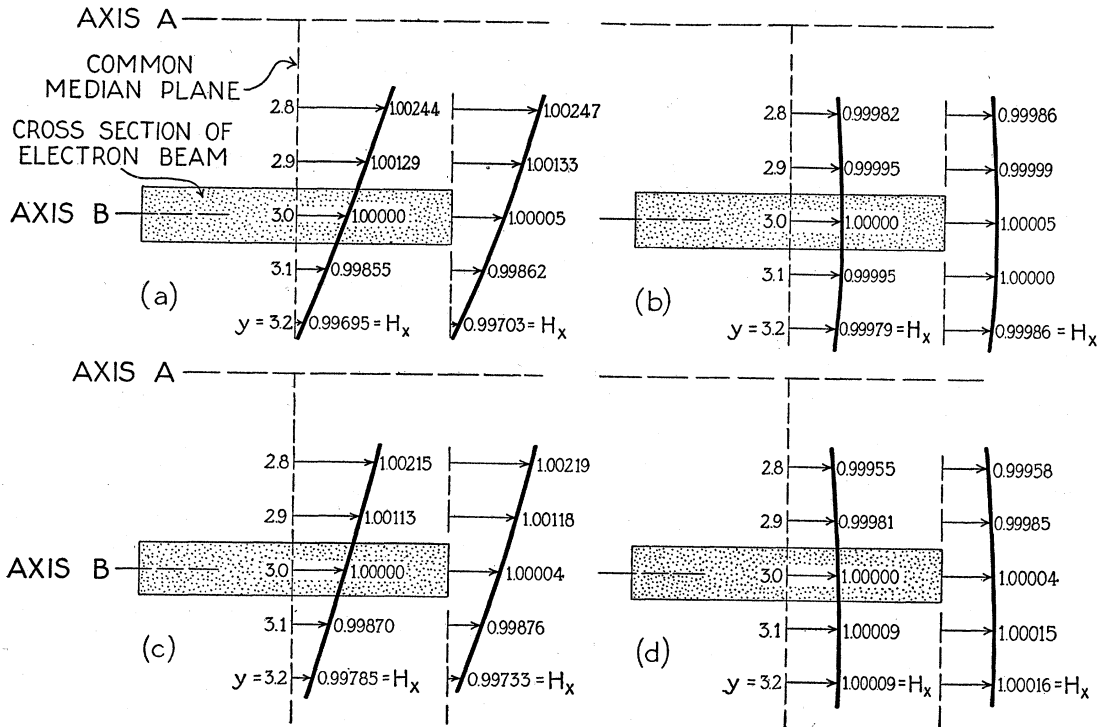


FIG. 7. Magnetic field intensity distribution diagrams, which show the intensity variation over the region in space traversed by the electron beam. The axes *A* and *B* refer to Fig. 6. Diagrams (a) and (b) illustrate respectively the case for two circular turns computed according to the Helmholtz separation ($x=4.0000$) and the improved separation ($x=3.4883$). (c) and (d) illustrate respectively the case for standard coil No. 1 computed according to the Helmholtz theory and according to the author's method. The values of H_x represent absolute field intensities for unit current, and y is in cm. The width of the cross section of the electron beam has been exaggerated to facilitate representation.

coordinates at the center of the coil of radius a , and $r^2 = a^2 + x^2$.

In the Helmholtz arrangement, $(\partial^2 H_x / \partial x^2)_{y=0} = 0$ reveals the presence of a point at $x = a/2$, where $\partial H_x / \partial x$ is constant. Thus by combining two circular turns so that each contributes to the field at $x = a/2$, great uniformity is obtained along the axis at a point midway between the two turns.

In order to secure uniformity off the axis but in the common median plane of the two circular turns, the condition, $(\partial H_x / \partial y) = 0$, was examined for a new separation. To a first approximation only the first three terms of Eq. (13) were used. This gave

$$\partial H_x / \partial y |_{y=\rho} = x^6 + Ax^4 + Bx^2 - N = 0,$$

where A and B are constant coefficients and N is the constant term. If ψ is substituted for x^2 , this

reduces to

$$f(\psi) = \psi^3 + A\psi^2 + B\psi - N = 0$$

and as a first approximation $x = 3.58148$ cm for field constancy at a point off the axis, $y = \rho = 3.0$, the approximate radius of curvature of the beam. The convergence of the infinite series was not sufficiently rapid for three terms, hence it was necessary to compute the value of x to a higher degree of approximation. For this purpose, five terms were used, with the result that

$$\begin{aligned} \partial H_x / \partial y |_{y=\rho} = & x_1^{14} + A_1 x_1^{12} + B_1 x_1^{10} + C_1 x_1^8 \\ & + D_1 x_1^6 + E_1 x_1^4 + F_1 x_1^2 - N_1 = 0, \end{aligned}$$

where A_1, B_1, \dots, F_1 represent the new constant coefficients, N_1 is the new constant term and x_1 is the new value of the separation. As before, the determination of x_1 can be simplified by sub-

stituting $\psi_1 = x_1^2$, with the result that

$$f(\psi_1) = \psi_1^7 + A_1\psi_1^6 + B_1\psi_1^5 + C_1\psi_1^4 + D_1\psi_1^3 + E_1\psi_1^2 + F_1\psi_1 - N_1 = 0.$$

Since the value of x obtained from the three term series represents an approximation to the root of the five term series, the evaluation of ψ_1 was carried out by the method of Newton.¹⁰ When the first approximate root $x = x_1$ was taken to be 3.58148, succeeding values were obtained as follows: $x_2 = 3.49204$; $x_3 = 3.48887$; $x_4 = 3.48830$. The fourth approximation satisfies the original equation with a residue of 1 part in 1.5×10^6 . When applied to a coil consisting of two circular turns, this value of x is the distance at which each of the turns must be located with respect to the common median plane in order to secure uniform intensity at a distance $y = \rho$ off the axis of the coils. The corresponding x for the Helmholtz pair would be 4.0000. In Fig. 7(a) and (b) are shown the field intensities computed¹¹ for these two separations, as applied to two single circular turns. The intensity in the region $y = \rho = 3.0$, is referred to unit value by proper choice of current ratios. The variation of intensity along the median plane with the new separation is of the order of 1:5000, for a variation in y of ± 2 mm, whereas in the Helmholtz case the variation is 12 times as much. The field at the edge of the electron beam, ± 1 mm from the common median plane, is also very constant. Fig. 7(c) and (d) illustrate the case of standard coil No. 1. Even in this case, where the cross section is finite, it is apparent that the improved separation produces a more uniform field along the median plane and over the section of the beam than the corresponding Helmholtz arrangement.

(c) *Intensity constant for standard No. 1.*— In order to compute the constant for standard No. 1, we shall regard it as made up of a pair of coils, each composed of a set of seven coaxial circular turns of equal radii. The contribution of each of the seven pairs of turns, which are symmetrical about the common median plane,

was computed for $y = \rho$ by means of five terms of the infinite series (Eq. 13) and the separation used. The summation of these gave

$$H_{x(1)}|_{y=\rho} = 0.841651 \text{ oersted/ampere.} \quad (14)$$

An independent computation of the field was carried out by a new method of successive approximation¹² which confirms the sufficiency of the five terms previously used. This powerful, new method allows the absolute value of the field to be rapidly determined to any desired approximation.

The expression for field intensity at the point $y = \rho$ due to a single pair of circular turns of radius a and symmetrical about the common median plane at the improved separation used is

$$H_x|_{y=\rho} = 0.4\pi a i \bar{L} / \bar{A}^2$$

or for the seven symmetrical pairs,

$$H_x|_{y=\rho} = 0.4\pi a i \sum_{k=1}^7 \frac{\bar{L}_k}{\bar{A}_k^2},$$

where $\bar{A} = \lim A_j = \lim B_j$;

$$\bar{L} = \lim L_j = \lim M_j;$$

$$A_{j+1} = \frac{A_j + B_j}{2}; \quad B_{j+1} = (A_j B_j)^{\frac{1}{2}};$$

$$L_{j+1} = \frac{L_j + M_j}{2}; \quad M_{j+1} = \frac{B_j L_j + A_j M_j}{2B_{j+1}};$$

and $A^2 = (LA)^2 + x^2$; $B^2 = (MB)^2 + x^2$,

where $LA = a + \rho$ and $MB = a - \rho$.

In this way the contributions of each of the seven symmetrical pairs were computed to an approximation better than 1:10⁶, with the result that the constant for standard No. 1 by this method is

$$H_{x(1)}|_{y=\rho} = 0.841591 \text{ oersted/ampere.} \quad (15)$$

The agreement between this value of H_x and that obtained by straightforward summation (Eq. 14) of the five term infinite series is about 1:14,000. Thus, terms beyond the fifth may be disregarded. When four terms of the series are used, the difference is 1:5000.

¹² This method is due to Dr. W. Bartky to whom I express my gratitude.

¹⁰ Scarborough, *Numerical Mathematical Analysis* (Johns-Hopkins Press, 1930), p. 178.

¹¹ I take this opportunity to express my great appreciation of the valuable aid rendered by Dr. P. G. Saper throughout the entire work of computing the magnetic field.

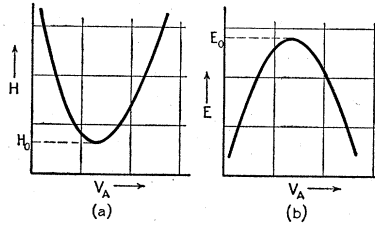


FIG. 8. Theoretical curves which show the variation, (a) in the magnetic field and, (b) in the electric field that is required in order to focus when the electron velocity is varied.

(d) *Intensity constant for standard No. 2.*— Thus far, no mention has been made of the helical nature of the current flowing in the various coils. The computations were based on the assumption that each turn of standard No. 1 was a circular turn.

In order to determine the effect of a helical current the constant of standard No. 2 was evaluated in terms of the line integral of the magnetic intensity taken around the helix which constituted this standard. The element of intensity for a point in the axis but off the common median plane is

$$dH_{x(2)} = a^2 i d\theta / [a^2 + (\chi - p\theta)^2]^{\frac{3}{2}}, \quad (16)$$

where a is the radius of the coil, $2\pi p$ the pitch, χ the distance from the reference plane to the point at which the field is expressed and $d\theta$ is the angle subtended on the axis by the normal component of the current element. The limits of integration are derived from the pitch and the number of turns on the coil. For the present computation, the limits were referred to the common median plane. Under these conditions, Eq. (16) reduces to

$$H_{x(2)} = \frac{4.8\pi i}{[a^2 + (24p\pi)^2]^{\frac{3}{2}}}. \quad (17)$$

Upon substituting numerical values,¹³ the constant for standard No. 2 in its axis becomes

$$H_{x(2)} = 0.843923 \text{ oersted/ampere.}$$

When standard No. 1 was compensated by

¹³ It is noteworthy that when $p=0$, Eq. (17) reduces to the standard form where the winding is assumed concentrated into a group of plane circular filaments. The field intensity computed from this arrangement exceeds by 14 : 10,000 the intensity determined from Eq. (17).

standard No. 2

$$H_{x(1)}|_{y=p} = 0.841480 \text{ oersted/ampere.} \quad (18)$$

(e) *Intensity constant for magnetic field coils.*— Of the three values obtained for $H_{x(1)}$, as revealed by Eqs. (14), (15) and (18), the value from Eq. (15) supersedes that given by Eq. (14) since it is a closer approximation than the evaluation of the five terms of the infinite series. Furthermore, with the present arrangement of apparatus, it was more desirable to determine the constant of the magnetic field coils by the use of standard No: 1. Hence, for present purposes, standard No. 2 served merely as an experimental check on standard No. 1 with a resultant agreement of approximately 1 : 8000. For this reason, the constant of the magnetic field coils was computed in terms of Eq. (15) with the result that

$$H_{x(m)} = 10.6291 \text{ oersted/ampere.}$$

In connection with the above method of compensation¹⁴ for the determination of the constant of the magnetic field coils, it is important to recall that the intensity distribution diagrams shown in Fig. 7 were arrived at by computation. However, when standard No. 1 was used to determine the constant of the magnetic field coils, compensation occurred in the region of space occupied by the magnetometer. Since the cross section of the magnetometer was comparable with the cross section of the electron beam, it has been assumed that the constant of the magnetic field coils, as so determined, represented the field over this region. This is a reasonable assumption because an equally homogeneous intensity distribution would be expected for the magnetic field coils. As a matter of fact, Lyle¹⁵ has shown that, as far as its external field is concerned, a circular coil of finite section can be replaced by one or more equivalent circular turns. Thus the theory, exemplified by Fig. 7(b), can be applied very simply to the equivalent pair of circular turns of a double coil of finite section in order to improve the uniformity for points off the axis.

¹⁴ In order to anticipate the thermal expansion of the coils and their supports due to the heating effect of the field current, compensation was carried out by means of appropriate current intensities after the normal current required to excite the field coils had produced thermal equilibrium. No effect due to this could be detected.

¹⁵ Lyle, *Phil. Mag.* **3**, 310 (1902). Cf. also Barnett, *Research Dept. Terr. Mag., Carnegie Inst.* **4**, 382 (1921).

IV. EXPERIMENTAL RESULTS

(A) Focusing criteria

Although Eq. (12) does not require that the electron velocity be determined in order to find e/m , only electrons of a certain voltage equivalent will reach the collector with given values of electric and magnetic fields. Let us consider the case of the dependence of the path upon the velocity only, and suppose the beam to have no divergence, that is $c_1=0$ in Eq. (9). Suppose further that the slit and collector are adjusted to the same distance from the center ($c_0=0$). Then at the collector, $r=\rho(1+\delta^2)$, where the velocity of the rays is defined in terms of δ by $v=\rho\theta_0' = \frac{1}{2}H\rho(1+\delta)e/m$. Thus the beam reaches the collector at the minimum distance ρ when $\delta=0$, or $v=\frac{1}{2}H\rho e/m$. Introducing the accelerating potential V_A in place of the velocity v , and substituting for $H\rho$ in Eq. (12), we find

$$V=2V_A \log_e (r_2/r_1). \tag{19}$$

This value of V_A gives a minimum value to r so that a slight variation in V_A moves the beam outward a very small amount.

In order to determine experimentally the electron velocity which must be employed with given electric and magnetic fields, we combine the two equations, $mv^2/\rho=Hev-Ee$ and $\frac{1}{2}mv^2=eV_A$, and solve for H with the result that

$$H = \frac{2V_A + \rho E}{\rho(2V_A e/m)^{1/2}},$$

where E is the electric field intensity, H is the magnetic field intensity, ρ is the radius of curvature and V_A is the accelerating potential applied between the filament and the slit. This potential

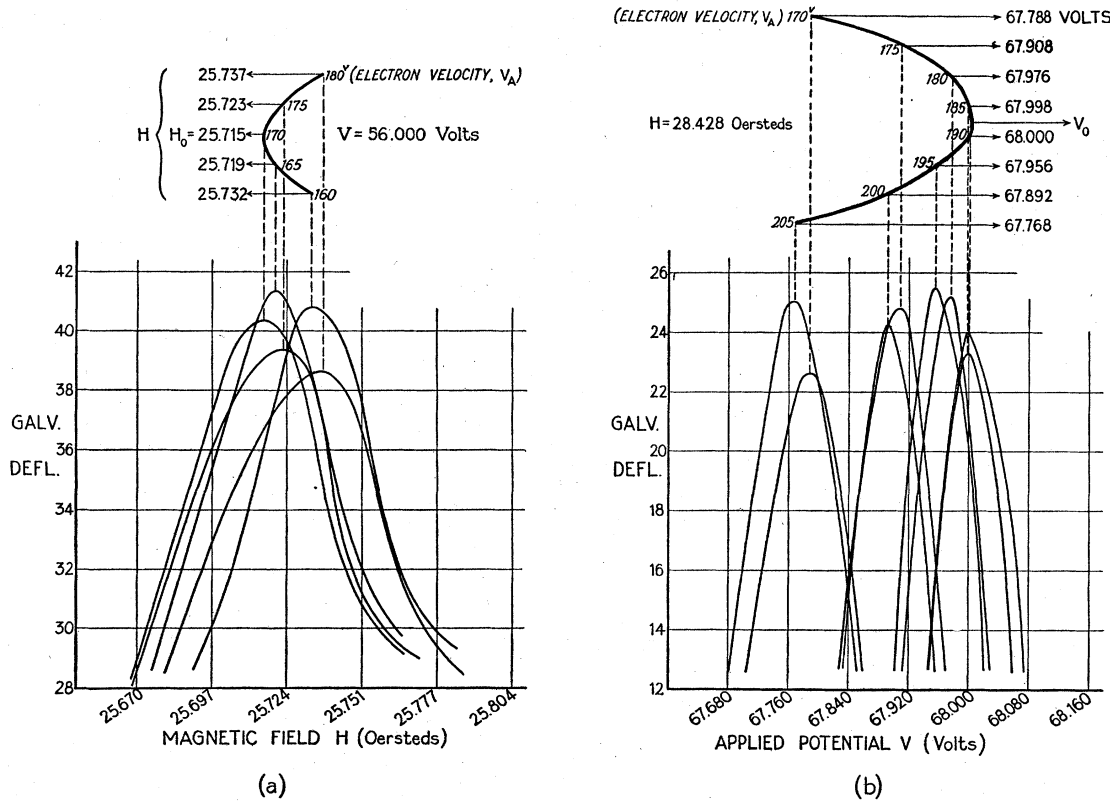


FIG. 9. Curves which show experimental results of test of focusing criteria. The sharpness of the focus increases slightly toward H_0 and V_0 and the focusing curve of maximum sharpness occurs in the magnetic case at H_0 and in the electric case at V_0 . The width of the curve of maximum sharpness in both cases is slightly less than the theoretical width computed from the dimensions of the slit and the collector.

is measured externally by means of a precision megohm voltmeter (V_A in Fig. 2).

The curve shown in Fig. 8(a) represents the general form of the variation of H with V_A . This curve is the locus of the maxima of the individual focusing curves, each of which corresponds to a particular electron velocity and each is obtained by variations of H while that particular velocity is kept constant. It is to be understood, in obtaining the focusing curves, that E is constant when H is varied through the turning point in the curve which corresponds to the particular velocity.

In a similar manner, we get

$$E = [H\rho(2V_A e/m)^{1/2} - 2V_A]/\rho.$$

Fig. 8(b) shows the general form of the variation of E with V_A . In this case, the focusing curves are secured by varying the electric field intensity for a particular electron velocity at a constant magnetic field intensity.

Each of the curves shown in Fig. 8 reveals a unique value of the velocity V_A corresponding to particular values of electric or magnetic field intensity, namely H_0 and E_0 . From $(\partial H/\partial V_A) = 0$, we get, $V_A = \rho E/2$, at $H = H_0$; and from $(\partial E/\partial V_A) = 0$, $V_A = (H^2 \rho^2 e/m)/8$, at $E = E_0$. When these values of V_A are substituted into their respective equation for H or E , the equation for e/m , in either case, becomes, $e/m = 4E/H^2\rho$. The radial electric field intensity E is now expressed in terms of the applied potential V , and e/m reduces to

$$e/m = \frac{4V}{H^2 \rho^2 \log_e (r_2/r_1)}.$$

This equation for e/m corresponds to the unique velocity V_A associated with the turning points where $E = E_0$, when H is constant, or where $H = H_0$, when E is constant. Thus e/m is expressed in terms of a magnetic field intensity and an electric field intensity for a unique electron velocity V_A . Hence we see that in order to bring a beam of electrons to focus under the action of given electric and magnetic forces, the electrons must possess a unique velocity V_A , as defined by the foregoing criterion, even though this velocity does not enter the equation for e/m .

In Fig. 9 are shown typical results of the ex-

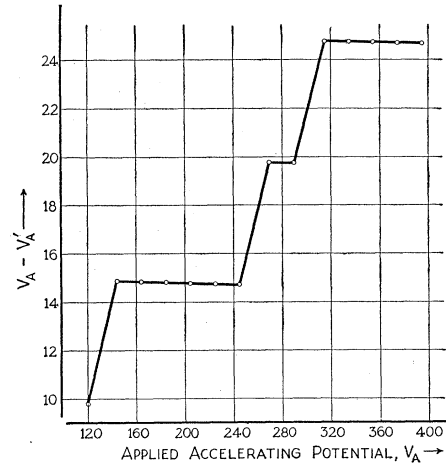


FIG. 10. Curve showing differences between the energy of the electrons before and after emergence from the slit (S in Fig. 3). The differences increase in approximately 5 volt steps.

perimental test of the focusing criteria. The group of curves plotted in Fig. 9(a) with galvanometer deflection against magnetic field intensity H are the actual focusing curves. Each of the focusing curves was taken at the particular velocity indicated on the single curve shown above them in the figure. This single curve is the locus of the maxima of the focusing curves. Thus we have at the point corresponding with $H = H_0$ a magnetic field intensity of 25.715 oersted, a constant potential V of 56.000 volts across the electric field plates and an electron velocity of 170 volts, as applied and measured externally by V_A in Fig. 2. The group of curves shown in Fig. 9(b) illustrates the situation for a variation of the electric field. In this case, the focusing curves were secured by varying the potential V across the electric field plates for a constant magnetic field $H = 28.428$ oersteds, with a particular electron velocity corresponding to each focusing curve. For this family of curves, $V_0 = 67.999$ volts.

It is evident from Fig. 9 that quite an appreciable uncertainty can exist in the evaluation of the electron velocity associated with the points $H = H_0$ or $E = E_0$, without affecting the determination of H_0 or E_0 . For example, if the electron velocity were uncertain to the extent of ± 2 volts, at the point $H = H_0$, the maximum uncertainty in the magnetic field would not exceed 1:6000. However, the velocity associated with the

point $H=H_0$, or $E=E_0$, is merely incidental as far as the computation of e/m is concerned. The ultimate precision of the determination of e/m is related to the accuracy with which H_0 or E_0 can be ascertained from the so-called locus curves and is independent of the corresponding velocities. In other words, the focusing criteria developed above serve merely as an experimental device for selecting particular electron velocities which can be focused with given electric and magnetic field intensities.

(B) Magnitude and origin of the differences between experimental and theoretical values of V_A

The actual determination of e/m was carried out for a wide range of electric and magnetic field intensities, where the corresponding velocities varied from 120 to 400 volts. It is important to observe that the values of V_A that were required to give the adjustment for minimum $r=\rho$, did not agree with the values computed from Eq. (19). To illustrate the differences noted, it was found experimentally, for example, that for a given value of V and H , the value of V_A was 120 volts, as measured by the megohm voltmeter (V_A in Fig. 2), whereas from Eq. (19), V_A should have been 110 volts. Likewise for a higher value, V_A was 245 volts by measurement and only 230 volts by computation. Throughout the entire range of readings there was a difference between the value of accelerating potential measured experimentally and the value obtained by theoretical computation. This difference depended upon the magnitude of the applied accelerating potential, and was greater for the higher accelerating potentials. Curiously enough, the increase in this difference for increasing values of accelerating potential took place in approximately five volt steps. In order to distinguish these two potentials, we shall let V_A be the applied accelerating potential, as measured experimentally, and V_A' be the effective value obtained with the actual focusing data by theoretical computation from Eq. (19).

Figure 10 illustrates the variation in this difference as a function of the applied accelerating potential V_A . In Fig. 10, the axis of abscissas represents the applied accelerating potential, as measured externally by the megohm volt meter,

and the ordinates are the differences between the applied accelerating potential and the effective accelerating potential, as defined by Eq. (19). We might think of the effective accelerating potential as the equivalent electron velocity associated with the electrons after they have emerged from the slit into the region of the deflecting fields. The applied accelerating potential, on the other hand, is the actual potential applied between the filament and the slit. Theoretically, these two velocities should be identical. However, it appears as if there existed in the neighborhood of the slit a retarding field which slowed down the electrons before they emerged from the slit. As a result of this retardation, the emergent electrons possessed the critical velocity required for focusing by the particular electric and magnetic forces operating. The velocity of the emergent electrons is expressed by Eq. (19) and the difference between this potential and the applied potential is a measure of the retarding field present. This retarding field may arise from an electronic charge which accumulates on the surface of the slit adjacent to the filament. That direct electron bombardment may modify a metal surface sufficiently to sustain a floating charge was pointed out in an earlier paper.¹

From the foregoing, we infer the significant fact that in the method of crossed electric and magnetic fields the focusing is carried out with electrons whose effective velocity after emergence from the slit is known precisely from the electric and magnetic forces operating. Therefore, any retardation experienced in the region of the slit does not constitute an uncertainty in this method of measuring e/m . Since practically all other experimental methods that are used for the determination of e/m by electron deflection depend in one way or another upon a knowledge of the velocity of the electrons, the existence of this effect presents a serious difficulty in the use of these other methods.

(C) Attempts of Kirchner and Dunnington to correct for velocity uncertainties

Apparently the only correction which Kirchner¹⁶ attempted to make for a possible velocity uncertainty was the correction for the contact

¹⁶ F. Kirchner, Ann. d. Physik 12, 503 (1932).

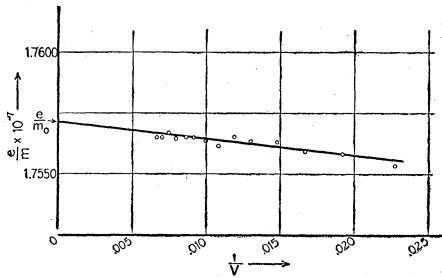


FIG. 11. Curve showing variation of the calculated value of e/m with the potential applied across the plates of the cylindrical condenser. $e/m_0 = kV'$; $e/m = kV$ and $e/m = e/m_0(1 + \xi/V)$, where $k = 4 \times 10^7 / H^2 \rho^2 \log_e (r_2/r_1)$. $V = V' + \xi =$ applied potential; $V' =$ actual deflecting potential and $\xi =$ surface polarization layer, in volts. The data shown were taken under the following conditions; 24-carat gold surfaces on cylindrical condenser; $p = 5 \times 10^{-7}$ mm Hg. i (collector) $= 1.8 \times 10^{-10}$ amp.; $\rho = 3.0971$ cm; $\log_e (r_2/r_1) = 0.199787$; $\xi = 0.069$ volt.

potential difference between the hot cathode and the slit in his apparatus. Measurements were made of the electron emission at various temperatures over a potential range from 0 to 10 volts, between the hot cathode and the center of the brass anode. On the assumption of the validity of the $V^{3/2}$ law at these low voltages, a plot was made of I against V . The result was a curve which possessed a negative intercept on the voltage axis. This intercept was of the order of 1.5 volts and was interpreted by Kirchner as due to the contact P.D. between the hot cathode and the slit. This whole procedure depends upon the questionable assumption of the validity of the three-halves power law at low voltages. Volta potentials have been measured¹⁷ by a scheme similar to this, but under circumstances which more closely approximated the assumptions of the theory. Furthermore, this method of correction does not take into account the presence of the space charge or polarization layer discussed under (B). Since the magnitude of the polarization layer depends upon the accelerating potential, it should be rather appreciable in Kirchner's experiment, where the accelerating potentials ranged from 1000 to 2000 volts.

The final equation employed by Dunnington¹⁸ for the computation of e/m by his method appears to be independent of the velocity of the electrons. However, his elaborate experiments revealed

that if the gold surfaces of the deflecting chamber and the slit system had suffered electron bombardment for fifteen hours or so, the subsequent values of e/m were appreciably altered. This difference was attributed to the formation of a polarization layer under direct electron bombardment. In order to correct for these polarization layers or surface charges, Dunnington assumed they were constant (constant emission current and small lapse of time). Hence extrapolation to infinite electron energy gave a corrected value of e/m .

In previous experiments,¹ the polarization layer which formed on the plates of the electrostatic field was found to be constant for a matter of hours, *provided no direct electron bombardment of the plates occurred. In the present paper it is shown that the layers formed under direct electron bombardment were not constant, but depended upon the velocity.* Furthermore, they appeared to be formed almost instantaneously and preliminary tests revealed the interesting fact that they were reversible. The accelerating potential in Dunnington's experiment is derived from the high frequency field, therefore, one would not expect the surface layers to be constant under these circumstances. There is also considerable possibility of such layers occurring on all the slits in Dunnington's apparatus with a consequent uncertainty in the electron energy and a distortion of the orbit.

(D) Determination of e/m

It was found most convenient to focus by varying the magnetic field for a constant electric field, since it was much easier to maintain the electric field constant than to maintain the magnetic field constant. The group of magnetic focusing curves shown in Fig. 9(a) constitutes one set of data for the calculation of e/m . In this case e/m would be expressed in terms of $H_0 = 25.715$ oersted, $V = 56.000$ volts, the average radial position of the slit and the collector, and the radii of the two condenser plates. However, the curves in Fig. 9 are merely typical, experimental curves which were taken during the investigation of the focusing theory. After the preliminary work on the focusing theory had been completed, the apparatus was very carefully gold plated again and then measured physically, after which several final sets of data were taken over a wide

¹⁷ W. Schottky, Ann. d. Physik **44**, 1011 (1914).

¹⁸ F. Dunnington, Phys. Rev. **52**, 475 (1937).

range of electric and magnetic field intensities. In the actual evaluation of e/m from these data, the peak values of the focusing curves could be ascertained without the necessity of plotting the focusing curves themselves. From the simple locus of these peak values, the values of H_0 were determined with considerable accuracy, as can be judged from the curves in Fig. 9. It is interesting to observe that in the process of collecting the final data, it was possible to repeat readings of the peak values of the focusing curves to better than 1 : 10,000.

The computation of e/m for the entire range of field intensities investigated revealed the dependence of the computed value upon the potential applied across the plates of the cylindrical condenser, as pointed out in an earlier paper.¹ The graph in Fig. 11 shows the variation of e/m with this potential. It is very important to recall that the surface polarization layer formed on the electric field plates is constant for: (1) a given intensity of electron beam; (2) constant gas pressure; and (3) clean metal surfaces, *provided no direct electron bombardment of these plates is allowed to occur during the process of focusing the beam*. In order to accomplish this, a shift to a new pair of electric and magnetic intensities was made only after the applied accelerating potential had been reduced to zero (see switch S in Fig. 2). In this way the electrons were kept out of the region between the electric field plates until the new set of field values had been adjusted approximately to bend the electrons into a circular orbit. After this preliminary adjustment, the focusing process was carried out with the beam deviating very little from the central circular orbit.

The final value of the specific charge was evaluated¹⁹ from the data of Fig. 11, by the

¹⁹ I wish here to express my appreciation to Mrs. Ardis T. Monk for checking independently the final results of the computation of e/m .

method of least squares, with the result that

$$e/m_0 = (1.7571 \pm 0.0013) \times 10^7 \text{ e.m.u.},$$

where the probable error is identified with the least squares solution.

Because of the physical limitations of the present cylindrical condenser, no attempt was made to push this determination to the extreme limits of accuracy attainable with this new method. However, the very slight eccentricity of the electric field plates does not invalidate the probable error stated.²⁰

In view of the work completed up to the present time, it is of interest to make a conservative estimate of the ultimate precision that should be attainable with this new method. From the self-consistency obtained in both the theoretical and the experimental evaluation of the magnetic field intensity, 1 : 6000 is a conservative estimate of the accuracy with which the magnetic field intensity can be determined. The present limitation of the cylindrical condenser is mainly physical. This uncertainty will be reduced considerably with a new condenser designed along kinematic lines. The radius of curvature of the beam must be measured to 0.005 mm in order to be known to within 1 : 3000. Previous measurements suggest that this should present no difficulty. The constants of the standard cells, standard resistances and the volt box are well within the projected limit of 1 : 3000. It is, therefore, the confident and conservative hope of the author that with the new cylindrical condenser a determination of e/m will be possible to within a probable error of 1 : 3000.

It is a great pleasure to express my appreciation to Dr. A. J. Dempster for his very generous interest during the course of this work.

²⁰ I am very grateful to Dr. Carl Eckart for an interesting discussion of this point.

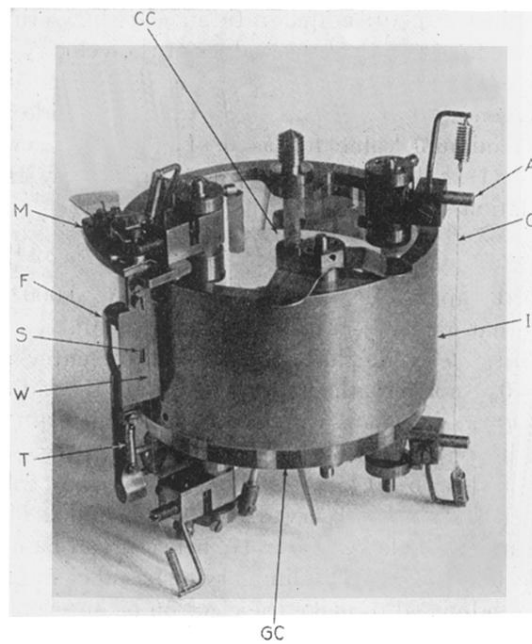


FIG. 3. Inner plate of cylindrical condenser, showing collector and slit system. *C*, gold wire collector, 0.045 mm diameter; *A*, 0.1 mm pitch adjusting screw; *I*, inner plate of cylindrical condenser; *GC*, accurate glass cylinder; *CC*, center of curvature of plates engraved on front face of *GC*; *S*, slit for beam, 0.03×2.0 mm; *M*, mechanism for adjusting slit; *W*, old wire slit, no longer used; *F*, filament support. Filament is directly in back of *S*; *T*, spring to compensate for expansion of filament.

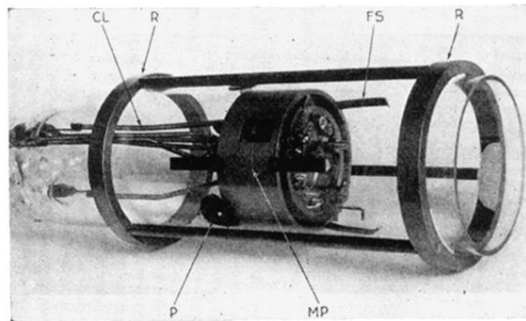


FIG. 4. Cylindrical condenser in glass tube. End plate removed. *CL*, spring connecting leads; *R*, ring supports; *MP*, median plane of electron beam; *P*, round glass pins that hold condenser in median plane under force of spring leads; *FS*, flat spring, of which there are six, to support condenser in glass tube.

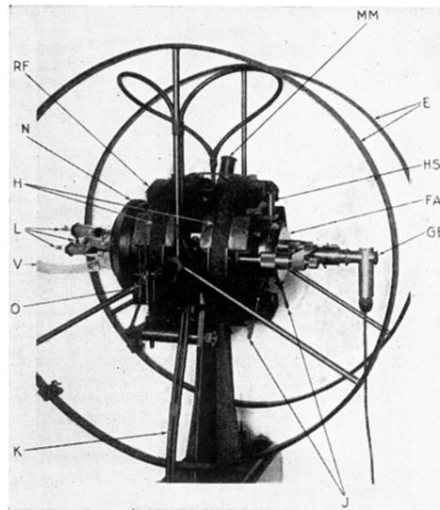


FIG. 5. Complete assembly of the entire apparatus with measuring microscopes in place. *FA*, glass tube containing cylindrical condenser; *E*, coils for investigating influence of earth's field; *GE*, combination Gauss eyepiece and telescope for locating cylindrical condenser; *J*, thumb screws to adjust position of cylindrical condenser—there are two in front and two in rear; *HS*, spring plunger which maintains glass tube (*FA*) in contact with thumb screws (*J*); *N*, nut to translate glass tube (*FA*) along axis of magnetic field; *MM*, median plane microscope to judge coincidence of median planes; *H*, magnetic field coils; *K*, noninductive connections to magnetic field coils; *RF* heat radiating fins; *L*, external leads for connections to cylindrical condenser, filament, etc.; *V*, vacuum pump connection; *O*, magnetometer mounted externally to indicate presence of stray fields.